

Local Instability of a Rotating Flow Driven by Precession of Arbitrary Frequency

Naing, Me Me

Faculty of Mathematics and Mathematical Research Center for Industrial Technology, Kyushu University

Fukumoto, Yasuhide

Faculty of Mathematics and Mathematical Research Center for Industrial Technology, Kyushu University

<https://hdl.handle.net/2324/16891>

出版情報 : MI Preprint Series. 2010-14, 2010-03-26. 九州大学大学院数理学研究院
バージョン :
権利関係 :



MI Preprint Series

**Kyushu University
The Global COE Program
Math-for-Industry Education & Research Hub**

Local Instability of a Rotating Flow Driven by Precession of Arbitrary Frequency

**Me Me Naing &
Yasuhide Fukumoto**

MI 2010-15

(Received March 26, 2010)

Faculty of Mathematics
Kyushu University
Fukuoka, JAPAN

Local Instability of a Rotating Flow Driven by Precession of Arbitrary Frequency

Me Me Naing and Y Fukumoto^{1‡}

Faculty of Mathematics and Mathematical Research Center for Industrial Technology, Kyushu University, 744 Motooka, Nishi-ku, Fukuoka, 819-0395, JAPAN

E-mail: mmnaing@math.kyushu-u.ac.jp

Abstract. We revisit the local stability, to three-dimensional disturbances, of rotating flows with circular streamlines, whose rotation axis executes constant precessional motion about an axis perpendicular to itself. In the rotating frame, the basic flow is steady velocity field linear in coordinates in an unbounded domain constructed by Kerswell (1993), and admits the use of the WKB method. For small precession frequency, we recover Kerswell's result. A novel instability is found at large frequency for which the axial wavenumber executes an oscillation around zero; drastic growth of disturbance amplitude occurs only in an extremely short time interval around the time where the axial wavenumber vanishes. In the limit of infinite precession frequency, the growth rate exhibits singular behavior with respect to a parameter characterizing the tilting angle of the wave vector.

Keywords: rotating flow, local stability, precession, Coriolis force

[‡] Corresponding author: yasuhide@math.kyushu-u.ac.jp

1. Introduction

The elliptical instability has been established as a universal mechanism for local instability of a rotating flow, with elliptically distorted streamlines, to three-dimensional disturbances of short wavelength. Bayly (1986) revealed that the stability problem of a velocity field linear in coordinates can be reduced to a system of ordinary differential equations. As a consequence, a general solution of the Euler equations linearized in disturbance amplitude is a linear superposition of the Floquet modes, and the growth rate is given by the exponents of a matrix Floquet problem. A thorough asymptotic analysis was implemented by Waleffe (1990). As an extension of Bayly's analysis, the geometric optics (WKB) method for time-evolution of localized disturbances on a general flow was developed (Friedlander and Vishik 1991, Lifschitz and Hameiri 1991) and now becomes a standard tool for studying local stability. A stability criterion is supplied by the solution of the initial-value problem of a system of the characteristic equations.

The stabilizing and destabilizing effect of the Coriolis force on the elliptical instability was studied for the case of the axis of the rotating frame being parallel to the vorticity vector of the basic flow relative to it, (Craik 1989, Miyazaki 1993, Fukumoto and Miyazaki 1996).

Understanding of response of rotating flows to precession has attracted attention from the viewpoints of planetary flows, dynamo and stability of spinning spacecraft containing a liquid (Meunier *et al.* 2008). In case the precession axis is perpendicular to the rotating axis of the basic flow, there are two types of precessing flows, with velocity field linear in coordinates and with streamlines of the relative flow projected to the plane normal to the rotation axis being of circular shape (Kerswell 1993, Mahalov 1993). In the rotating frame, these flows are realizable as a steadily rotating flow, subjected to the external Coriolis force, imposed by linear straining field of different types. The local stability of one of these flows was examined by Kerswell (1993), under the restriction that the precession frequency ϵ is small in magnitude compared with the angular velocity of the main rotation. Mahalov (1993) addressed the global stability of the other flow, under the same restriction, and clarified occurrence of parametric resonance instability between Kelvin waves whose azimuthal wavenumber are separated by one. The local stability of the latter flow, which corresponds to the short-wave limit of the global stability, was examined by Me Me Naing and Fukumoto (2009). The both flows suffer from the local instabilities of precession origin, and the growth rate takes the common value of $5\sqrt{15}|\epsilon|/32$. Me Me Naing and Fukumoto (2009) investigated a combined influence of the Coriolis force and linear straining field, and found that the growth rate is larger for the case of precession about the minor axis than for that about the major axis. An asymptotic analysis was carried through with use of Mathieu's method (Ince 1956) as applied to the reduced system built in the framework of Bayly *et al.* (1996).

In the absence of the elliptical straining field, the both flows are exact solutions of the Euler equations and of the Navier-Stokes equations as well. Me Me Naing and

Fukumoto (2009) further entered into the regime of large precession angular frequency for Mahalov's flow, and uncovered a new instability mechanism; the most unstable mode occurs when the wave vector is perpendicular to the rotating axis of the flow and its growth rate coincides with the angular velocity of the flow rotation.

This paper focuses on Kerswell's flow and, in particular, on the local stability at large precession frequencies. If the geometric optics approximation is applied to Kerswell's flow, depending on the precession frequency and the initial tilting angle of the wave vector, there may emerge moments of vanishing axial component of the wave vector, at which the reduced equations obtained by the dependent-variable transformation of Bayly *et al.* (1996) break down. In such a case, we cannot use the reduction method in order to grasp stability characteristics for a wide parameter range. Concomitantly with this breakdown, a novel feature of the instability, which exhibits a marked difference from the case of Mahalov's flow in the limit of high precession frequency, shows up. Numerical calculation shows that, at the large value of precession frequencies, the growth rates are different between Mahalov's and Kerswell's flows. The growth rate of Kerswell's flow is larger, though evaluation of the high precession-frequency limit is not as yet completed. The way of disturbance amplification is entirely different. Disturbances on Mahalov's flow exhibit smooth exponential growth in time. A distinguishing feature of the instability of Kerswell's flow is that explosive amplification of disturbances takes place only in an extremely short time interval about the moment of vanishing axial wavenumber, being possibly a new type of instability.

The reduction method is feasible for small values of precession frequency and for the tilting angle of the wave vector away from $\pi/2$. We corroborate the instability result by Kerswell (1993) by applying Mathieu's method to the reduced Floquet problem. After stating a brief formulation of the WKB method and writing down the characteristic equations, along with the reduced ones, applicable for flows in a rotating frame in §2, we start with the local stability analysis for slow precession. By numerical calculation and an asymptotic analysis, we recover Kerswell's result and extend the asymptotic expansions. Section 4 makes an excursion to fast precession and manifest the new instability mechanism prevailing rotating flows for which axial wavenumber passes through zero in a period. Section 5 makes a comparison of Kerswell's with Mahalov's flows. The last section (§6) is devoted to an overview of and discussions on the results.

2. Formulation and WKB characteristic equations

Let us consider a precessing rotating flow, of infinite expanse, whose velocity field is linear in coordinates, with angular velocity equal to unity, and whose rotating axis itself is rotated about an axis perpendicular to itself, with angular frequency ϵ . Otherwise stated, we are concerned with local stability of a rotating flow subjected to an external Coriolis force.

We choose, as the basic state relative to the rotating frame, $\mathbf{U}(x, y, z) = (-y, x - 2\epsilon z, 0)$, the same one analyzed by Kerswell (1993). The flow is rotating about the z -axis

which is itself rotating at constant angular velocity ϵ about the x -axis. The precessional angular velocity is written vectorially as $\boldsymbol{\Omega} = (\epsilon, 0, 0)$. The basic flow is an exact solution of the Euler and even of the Navier-Stokes equations, augmented by the Coriolis force, for an arbitrary value of ϵ . We pose no restriction on ϵ . Calculation is made of the growth rate of three-dimensional disturbances of infinitesimal amplitude for both small and large values of precession frequency $|\epsilon|$. The emphasis is put on a demonstration of instability for large values $|\epsilon|$, the other extreme from Kerswell's result (1993). We assume that the fluid is inviscid and incompressible.

In the rotating frame, the basic rotating axis is maintained at the z -axis. The pressure varies along the z axis as $p = (x^2 + y^2)/2 + 2\epsilon^2 z^2 - 2\epsilon xz$. Incidentally Mahalov (1993) considered the basic flow $\mathbf{U}_{\text{Ma}}(x, y, z) = (-y, x, -2\epsilon y)$ for precessing rotating with the same precessional angular velocity $\boldsymbol{\Omega} = (\epsilon, 0, 0)$. The boundary condition and the imposed far field pressure would select a realizable local field. The local stability of Mahalov's flow was investigated in our previous investigation (Me Me Naing and Fukumoto 2009).

The disturbance is governed by the Euler equations augmented by the Coriolis force. Owing to the linear dependence, in coordinates, of the velocity profile of the basic flow, we may superimpose the following form of three-dimensional localized disturbance velocity \mathbf{u}' and pressure p'

$$[\mathbf{u}'(\mathbf{x}, t), p'(\mathbf{x}, t)] = \exp(i\mathbf{k}(t) \cdot \mathbf{x})[\mathbf{a}(t), \tilde{p}(t)], \quad (1)$$

on the basic flow, where $\mathbf{k}(t)$ is the time dependent wave vector (Bayly 1986). We are concerned with amplification or non-amplification of the amplitude $\mathbf{a}(t)$ and $\tilde{p}(t)$. These are substituted into the Euler equations and terms quadratic in disturbance amplitude are neglected. Then the linearized Euler equations are reduced to a coupled system of ordinary differential equations:

$$\frac{d\mathbf{k}}{dt} = -\mathcal{D}^T \mathbf{k}, \quad (2)$$

$$\frac{d\mathbf{a}}{dt} = \left(\frac{2\mathbf{k}\mathbf{k}^T}{k^2} - \mathbf{I} \right) \mathcal{D}\mathbf{a} - 2 \left(\boldsymbol{\Omega} \times \mathbf{a} - [(\boldsymbol{\Omega} \times \mathbf{a}) \cdot \mathbf{k}] \frac{\mathbf{k}}{k^2} \right), \quad (3)$$

together with the incompressibility condition

$$\mathbf{k} \cdot \mathbf{a} = 0, \quad (4)$$

where $k = |\mathbf{k}| = (k_1^2 + k_2^2 + k_3^2)^{1/2}$, \mathbf{I} is the 3×3 unit matrix, superscript T stands for taking the transpose, and \mathcal{D} is a 3×3 constant matrix defined by

$$\mathcal{D} = \left[\frac{\partial U_i}{\partial x_j} \right] = \begin{bmatrix} 0 & -1 & 0 \\ 1 & 0 & -2\epsilon \\ 0 & 0 & 0 \end{bmatrix}. \quad (5)$$

By using an overdot for differentiation in t , equation (2) is written in component wise

as $(\dot{k}_1, \dot{k}_2, \dot{k}_3) = (-k_2, k_1, 2\epsilon k_2)$ and equation (3) is written as follows:

$$\begin{bmatrix} \dot{a}_1 \\ \dot{a}_2 \\ \dot{a}_3 \end{bmatrix} = \frac{1}{k^2} \begin{bmatrix} A_{11} & A_{12} & A_{13} \\ A_{21} & A_{22} & A_{23} \\ A_{31} & A_{32} & A_{33} \end{bmatrix} \begin{bmatrix} a_1 \\ a_2 \\ a_3 \end{bmatrix}, \quad (6)$$

where

$$\begin{aligned} A_{11} &= 2k_1k_2, A_{12} = -k_1^2 + k_2^2 + k_3^2 + 2\epsilon k_1k_3, A_{13} = -6\epsilon k_1k_2, \\ A_{21} &= -k_1^2 + k_2^2 - k_3^2, A_{22} = -2k_1k_2 + 2\epsilon k_2k_3, A_{23} = 4\epsilon k_1^2 - 2\epsilon k_2^2 + 4\epsilon k_3^2, \\ A_{31} &= 2k_2k_3, A_{32} = -2k_1k_3 - 2\epsilon(k_1^2 + k_2^2), A_{33} = -6\epsilon k_2k_3. \end{aligned}$$

Equation (2) has the following general solution:

$$\mathbf{k} = (\sin \theta \cos t, \sin \theta \sin t, \cos \theta - 2\epsilon \sin \theta \cos t), \quad (7)$$

where θ is a constant close, if $|\epsilon| \ll 1$, to the inclination angle of the wave vector \mathbf{k} from the rotation (z -) axis. With this form, (3) serves as a matrix Floquet problem. For handling these characteristic equations, it may be expedient to employ variables introduced by Bayly *et al.* (1996) that reduce equations (2)-(4) to a two-component system of periodic coefficients with period 2π . We decompose vectors into components in the xy -plane denoted by subscript \perp and the scalar component parallel to the z -axis denoted by subscript \parallel and write

$$\mathbf{U} = \begin{bmatrix} \mathbf{U}_\perp \\ -2\epsilon y \end{bmatrix}, \quad \mathcal{D} = \begin{bmatrix} \mathcal{D}_\perp & 0 \\ 0 & 0 \end{bmatrix} \begin{bmatrix} -2\epsilon \\ 0 \end{bmatrix}. \quad (8)$$

This decomposition manifests a peculiar feature of the problem by rewriting (2) into

$$d\mathbf{k}_\perp/dt = -\mathcal{D}_\perp^T \mathbf{k}_\perp + 2\epsilon k_2, \quad dk_\parallel/dt = 2\epsilon \sin \theta \sin t. \quad (9)$$

The perpendicular component \mathbf{k}_\perp of \mathbf{k} decouples from the parallel component. Notably, the z -component k_\parallel of \mathbf{k} varies with time t , unlike the cases so far investigated. This is the source for an unusual behavior of the growing mode at large values of $|\epsilon|$.

Denote the amplitude of the disturbance vorticity to be $\mathbf{b} = \mathbf{k} \times \mathbf{a}$ and introduce new variables

$$p = \frac{k}{k_\perp} \mathbf{k}_\perp \cdot \mathbf{a}_\perp, \quad q = \frac{k}{k_\perp} b_\parallel, \quad (10)$$

where use has been made of $k_\perp = |\mathbf{k}_\perp|$. As a consequence, (2) and (3) are reduced to

$$\frac{d}{dt} \begin{bmatrix} p \\ q \end{bmatrix} = \begin{bmatrix} L_{11} & L_{12} \\ L_{21} & L_{22} \end{bmatrix} \begin{bmatrix} p \\ q \end{bmatrix}, \quad (11)$$

where the matrix entries are

$$\begin{aligned} L_{11} &= \frac{d}{dt} \log \frac{k_\perp}{k} - \frac{4\epsilon k_2 k_3}{k_\perp^2} + \frac{2k_3 \dot{k}_3}{k_\perp^2} + \frac{\dot{k}_3}{k_3}, \\ L_{12} &= \frac{2k_3^2}{k^2 k_\perp^2} \mathbf{k}_\perp^T \mathcal{H} \mathbf{k}_\perp + \frac{2\epsilon k_1 k_3}{k^2}, \\ L_{21} &= -\frac{1}{k_3} (2k_3 + 4\epsilon k_1), \quad L_{22} = -\frac{d}{dt} \log \frac{k_\perp}{k}, \end{aligned} \quad (12)$$

supplemented by

$$\mathcal{H} = \mathcal{D}_\perp \begin{bmatrix} 0 & 1 \\ -1 & 0 \end{bmatrix}.$$

The detail of calculation may be referred to Bayly *et al.* (1996) and Lifschitz (1994).

From equation (7), the magnitude $k_\perp = |\sin \theta|$ of the horizontal wave vector never vanishes unless $\theta = 0$. But the axial wavenumber k_\parallel passes through zero at the time t^* when $\cos \theta - 2\epsilon \sin \theta \cos t^* = 0$ is satisfied. Given θ ($0 \leq \theta \leq \pi$), this occurs twice per period if $\epsilon > \cot \theta/2$. Given ϵ of whatever small value in magnitude, $k_\parallel = 0$ occurs for $\theta_c < \theta \leq \pi/2$ with θ_c defined by $\cot \theta_c = 2\epsilon$. If $k_\parallel = 0$, L_{11} and L_{21} at least diverge and equation (11) is no longer validated. We have but to appeal to the original system (6) in order to draw stability diagram over a wide range of the parameter space (ϵ, θ) .

3. Influence of weak precession

This section is concerned with the case of a weak external Coriolis force. The Floquet method is directly applicable to the original equation (6). We apply the Floquet method to the original equation (6) and calculate numerically the stability boundary and contours of the growth rate in the parameter space (ϵ, θ) .

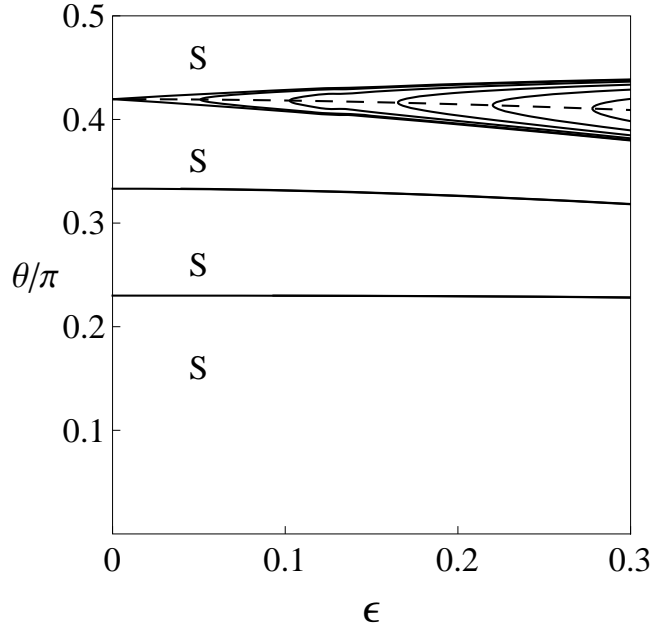


Figure 1. Contours of the growth rate, in the (ϵ, θ) plane, calculated from (6) for small values of ϵ ($0 \leq \epsilon \leq 0.3$). The stability region is marked with S. For given ϵ , the maximum growth rate is attained at the inclination angle θ shown by the dashed line. The boundary curves correspond to $\sigma = 0$. The increment of σ between neighboring contours is $\Delta\sigma = 0.2/2\pi$.

Figure 1 draws the contours of the growth rate for $\epsilon \leq 0.3$. The diagram is symmetric with respect to the θ -axis ($\epsilon \rightarrow -\epsilon$), The instability occurs between

the two solid lines. The stability region is marked with S. Three instabilities regions, emanating from $\theta = \cos^{-1}(1/4)$, $\cos^{-1}(1/2)$ and $\cos^{-1}(3/4)$, are identified. The uppermost instability band starts from $\theta = \cos^{-1}(1/4)$ ($\theta/\pi \approx 0.41956938$). Given ϵ , the largest growth rate occurs at the value of the inclination angle θ in the midway of the uppermost instability band, which is displayed with the dashed line.

For very small values of $|\epsilon|$, when expanded in powers of ϵ , (11) is approximated by the Mathieu equation:

$$\ddot{q} + (u + 2\epsilon a_1 \cos t)q = 0, \quad (13)$$

where

$$u(\theta) = 4 \cos^2 \theta, \quad a_1(\theta) = -3 \cos \theta \sin \theta + 8 \cos^3 \theta \sin \theta.$$

We invoke the Mathieu method (Ince 1956) to seek parametric resonance and to calculate its growth rate. First, we assume the solution of (13) in the following form:

$$q = e^{\sigma t} (\dots + b_{-\frac{3}{2}} e^{-\frac{3}{2}it} + b_{-\frac{1}{2}} e^{-\frac{1}{2}it} + b_{\frac{1}{2}} e^{\frac{1}{2}it} + b_{\frac{3}{2}} e^{\frac{3}{2}it} \dots).$$

With this form, (13) is converted to Hill's determinantal matrix form:

$$\begin{bmatrix} f_1 & \epsilon a_1 & 0 & 0 \\ \epsilon a_1 & f_2 & \epsilon a_1 & 0 \\ 0 & \epsilon a_1 & f_3 & \epsilon a_1 \\ 0 & 0 & \epsilon a_1 & f_4 \end{bmatrix} \begin{bmatrix} b_{-\frac{3}{2}} \\ b_{-\frac{1}{2}} \\ b_{\frac{1}{2}} \\ b_{\frac{3}{2}} \end{bmatrix} = \mathbf{0}, \quad (14)$$

where

$$\begin{aligned} f_1 &= \left(\sigma - \frac{3}{2}i \right)^2 + u, & f_2 &= \left(\sigma - \frac{1}{2}i \right)^2 + u, \\ f_3 &= \left(\sigma + \frac{1}{2}i \right)^2 + u, & f_4 &= \left(\sigma + \frac{3}{2}i \right)^2 + u. \end{aligned}$$

In the absence of the precession ($\epsilon = 0$), the requirement of vanishing determinant of the matrix in (14) provides the eigenvalues

$$\sigma^2 = - \left(\sqrt{u} \pm \frac{1}{2} \right)^2, - \left(\sqrt{u} \pm \frac{3}{2} \right)^2.$$

When the parameter $|\epsilon|$ is small in magnitude, the instability is possible only around $u = 1/4$ and $9/4$. We consider the effect of the small Coriolis force, to $O(\epsilon^4)$, on σ^2 .

- (i) at $u = \frac{1}{4}$ or $\cos \theta = \pm \frac{1}{4}$, $\sigma^2 = (\epsilon a_1)^2 - \frac{15}{4}(\epsilon a_1)^4$ or $\sigma \approx \frac{5\sqrt{15}}{32}|\epsilon|(1 - \frac{75}{64}\epsilon^2)$,
- (ii) at $u = \frac{9}{4}$, $\sigma^2 = -\frac{1}{36}(\epsilon a_1)^4$,

The latter indicates neutral stability to $O(\epsilon^2)$. The former is the subharmonic instability, being the primary mode of precession origin, with $\sigma \approx 5\sqrt{15}|\epsilon|/32$ at $\cos \theta = \pm 1/4$. Thus Kerswell's result (1993) is restored by the asymptotic analysis. In the slow precession limit, Kerswell's flow shares the same growth-rate value with Mahalov's flow (Me Me Naing and Fukumoto 2009).

Second, we pose an alternative form of the solution of (13) as

$$q = e^{\sigma t}(\dots + b_{-2}e^{-2it} + b_{-1}e^{-it} + b_0 + b_1e^{it} + b_2e^{2it} + \dots).$$

Upon substitution, equation (13) gives way to

$$\begin{bmatrix} h_1 & \epsilon a_1 & 0 & 0 & 0 \\ \epsilon a_1 & h_2 & \epsilon a_1 & 0 & 0 \\ 0 & \epsilon a_1 & h_3 & \epsilon a_1 & 0 \\ 0 & 0 & \epsilon a_1 & h_4 & \epsilon a_1 \\ 0 & 0 & 0 & \epsilon a_1 & h_5 \end{bmatrix} \begin{bmatrix} b_{-2} \\ b_{-1} \\ b_0 \\ b_1 \\ b_2 \end{bmatrix} = \mathbf{0}, \quad (15)$$

where

$$\begin{aligned} h_1 &= (\sigma - 2i)^2 + u, h_2 = (\sigma - i)^2 + u, \\ h_3 &= \sigma^2 + u, h_4 = (\sigma + i)^2 + u, h_5 = (\sigma + 2i)^2 + u. \end{aligned}$$

In order for a non-trivial solution $(b_{-2}, b_{-1}, b_0, b_1, b_2) \neq \mathbf{0}$ to be gained, the determinant of the matrix in (15) must be zero. When $\epsilon = 0$, the eigenvalue σ is obtained at once as

$$\sigma^2 = -u, -(\sqrt{u} \pm 1)^2, -(\sqrt{u} \pm 2)^2.$$

The instability possibly comes out only through $u = 0, 1$ and 4 , when the precession ($\epsilon \neq 0$) is called into play.

Performing expansions of σ^2 in powers of ϵ to $O(\epsilon^4)$, we have

- (i) at $u = 0$, $\sigma^2 = -2\epsilon^2 - \frac{25}{2}(\epsilon a_1)^4$,
- (ii) at $u = 1$ or $\cos \theta = \pm \frac{1}{2}$, $\sigma^2 = \frac{5}{36}(\epsilon a_1)^4$ or $\sigma \approx \frac{9\sqrt{5}}{32}\epsilon^2$,
- (iii) at $u = 4$, $\sigma^2 = -\frac{1}{144}(\epsilon a_1)^4$.

It is likely that no instability is admitted at $u = 0$ and $u = 4$. The instability is driven only at $u = 1$ for which $\cos \theta = \pm 1/2$ or $\theta = \pi/3$ and $2\pi/3$, and its growth rate is $\sigma \approx 9\sqrt{5}\epsilon^2/32$, being of second order in ϵ . This mode corresponds to the middle instability band issuing from about $\theta \approx \pi/3$ in figure 1. This band is narrower, with growth rate smaller by an order in ϵ , than the subharmonic instability band issuing from $\theta = \cos^{-1}(1/4)$.

4. Influence of strong precession

The method of reducing to the variables to p and q gets into trouble when k_3 becomes zero at some moment, in the sense that equation (10) is not invertible for \mathbf{a} and \mathbf{b} . For large value of $|\epsilon|$, $k_3 = 0$ necessarily occurs and use of the reduced amplitude equation (11) is forbidden, as suggested by divergences of L_{11} and L_{21} . We have no way but to appeal to the original amplitude equation (6), supplemented by (7).

Figure 2 shows the growth-rate contours calculated from (6) over a wider range of ϵ ($0 \leq \epsilon \leq 5$). As $|\epsilon|$ is increased, contours become rather involved. Given ϵ , the maximum value of Floquet exponent, as a function of ϵ , is shown up to as large as $\epsilon = 1000$, in figure 3. The angle θ at which the maximum exponent is attained is drawn in figure 4.

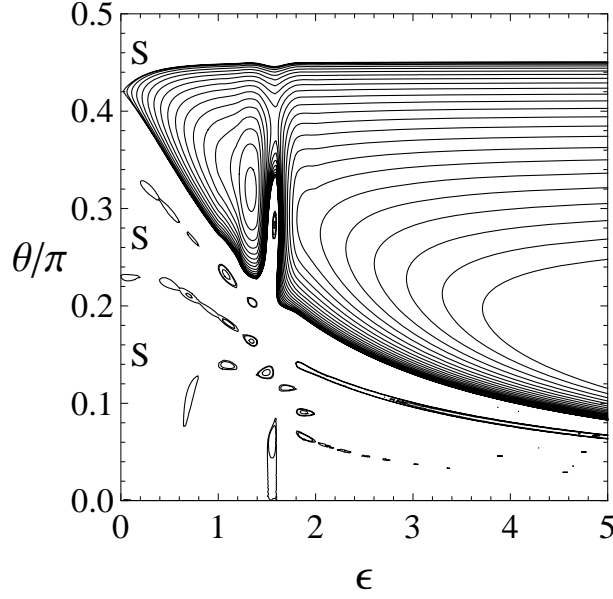


Figure 2. Contours of the growth rate, in the (ϵ, θ) plane, calculated from (6) for a wider range of ϵ ($0 \leq \epsilon \leq 5$). The stability region is marked with S. The boundary curves correspond to $\sigma = 0$. The increment of σ between neighboring contours is $\Delta\sigma = 0.2/2\pi$.

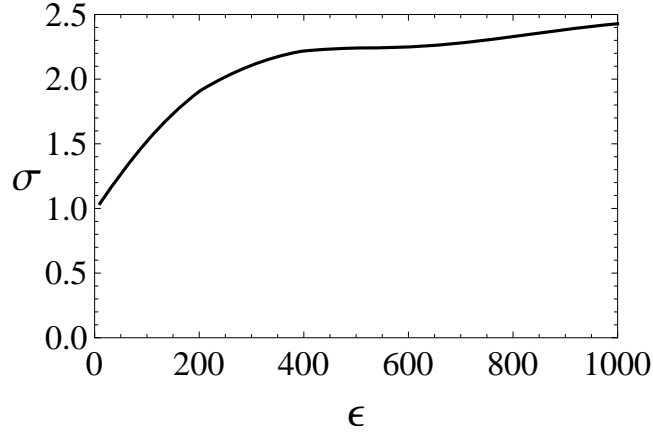


Figure 3. Maximum instability growth rate as a function of ϵ , calculated from (6).

We observe from figure 3 that the maximum growth rate increases monotonically with ϵ and that it exhibits a tendency of saturation. At this stage, it is hard to conclude whether σ tends to a finite value or not in the limit of $|\epsilon| \rightarrow \infty$. To have an idea of the amplification of the eigenfunction amplitude, we display, in figure 5, the x -component, $a_1(t)$ ($0 \leq t \leq 2\pi$), of the numerical solution for $\epsilon = 100$ and $\theta = 0.011983\pi$ of the most unstable mode. It is seen from figure 5 that the amplitude grows drastically during a very short time around t^* at which $k_3 = \cos\theta - 2\epsilon \sin\theta \cos t^* = 0$. This occurs at $t^* \approx 4.77601$ being consistent with figure 5. The zero of k_3 occurs twice in each period,

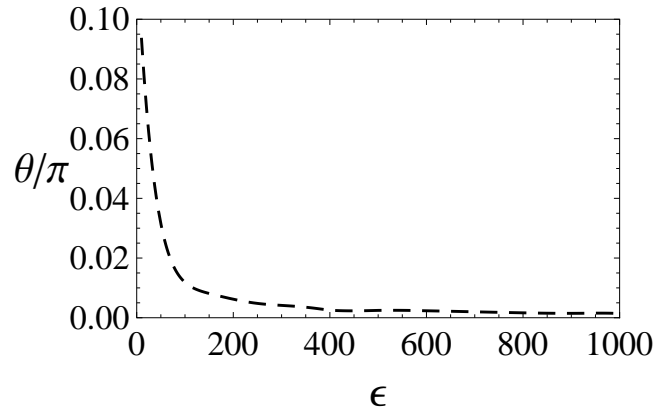


Figure 4. The inclination angle of maximum instability growth rate as a function of ϵ , calculated from (6).

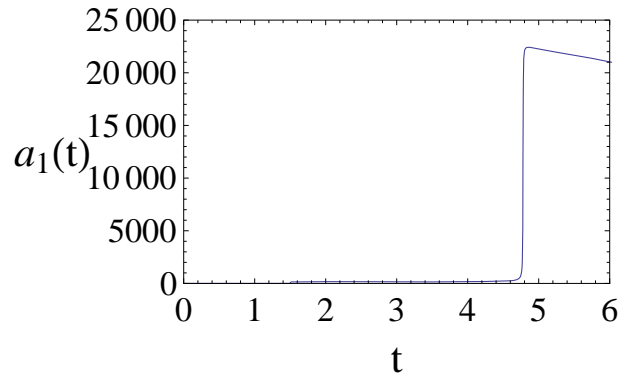


Figure 5. The x component of the solution of (6) for $\epsilon = 100$ and $\theta = 0.011983\pi$. During in a short time interval $a_1(t)$ growth rapidly.

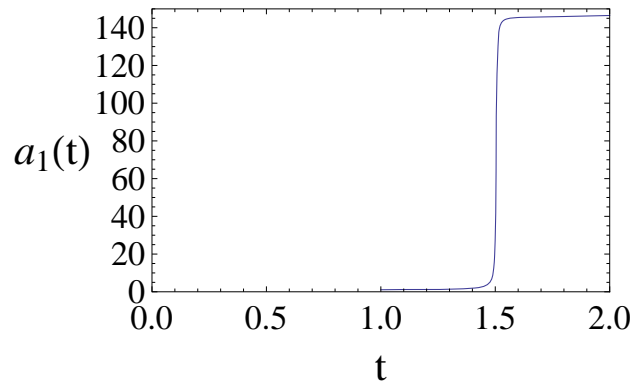


Figure 6. Close-up view of $a_1(t)$ around $t \approx 1.59493$.

and the other time is $t^* \approx 1.59493$. The same drastic growth around its moment t^* is observed as shown in figure 6.

As is read off from figures 5 and 6, the amplitude grows gradually in almost the whole period except for these short time interval around t^* . In order to answer the question of whether the growth rate is finite or not, it may suffice to estimate the solution, during the short time range centered on $t = t^*$. We will make an attempt to estimate the growth rate of the amplitude of the solution, with the aid of numerical results.

Consider the amplitude equations for the time ranges divided into two parts: the almost whole except for short time intervals around t^* and for the very short time. Since the largest growth rate occurs at $|\theta| \ll 1$ for $|\epsilon| \gg 1$, during the most of time except around $t = t^*$, the term proportional to $\epsilon \sin^2 \theta$ and $\sin^2 \theta$ are negligibly small compared with $|k_3|$ and $|k_3|^2$, and we may use a simpler version of the amplitude equation as

$$\begin{bmatrix} \dot{a}_1 \\ \dot{a}_2 \\ \dot{a}_3 \end{bmatrix} \approx \frac{1}{k_3^2} \begin{bmatrix} 0 & k_3 & 0 \\ -k_3^2 & 2\epsilon k_2 k_3 & 4\epsilon k_3^2 \\ 2k_2 k_3 & -2k_1 k_3 & -6\epsilon k_2 k_3 \end{bmatrix} \begin{bmatrix} a_1 \\ a_2 \\ a_3 \end{bmatrix}. \quad (16)$$

The situation is rather subtle when t comes close to t^* . During the extremely short time around $t = t^*$, $|k_3|$ becomes comparable with $|\theta|$ or even smaller than $|\theta|$ and therefore we must keep the terms proportional to $\sin^2 \theta$, $k_1 k_2$, k_1^2 and k_2^2 say, in the amplitude equation. Taking $\cos \theta \rightarrow 1$ and $\sin \theta \rightarrow 0$, equations (6) and (7) become

$$\begin{bmatrix} \dot{a}_1 \\ \dot{a}_2 \\ \dot{a}_3 \end{bmatrix} \approx \frac{1}{k^2} \begin{bmatrix} 0 & k_3 & -6\epsilon k_1 k_2 \\ -k_3^2 & 2\epsilon k_2 k_3 & 4\epsilon k_1^2 - 2\epsilon k_2^2 + 4\epsilon k_3^2 \\ 2k_2 k_3 & -2k_1 k_3 - 2\epsilon(k_1^2 + k_2^2) & -6\epsilon k_2 k_3 \end{bmatrix} \begin{bmatrix} a_1 \\ a_2 \\ a_3 \end{bmatrix}, \quad (17)$$

where the modulus of the wave vector is

$$k^2 = \sin^2 \theta + k_3^2. \quad (18)$$

By taking $\sin \theta \rightarrow \theta$ for the short moments around t^* , the wave vector becomes

$$\mathbf{k} \approx (\theta \cos t, \theta \sin t, 1 - 2\epsilon \theta \cos t), \quad (19)$$

$$k^2 \approx \theta^2 + k_3^2 = \theta^2 + (1 - 2\epsilon \theta \cos t)^2. \quad (20)$$

The amplitude equation (17) then gives way to

$$\begin{bmatrix} \dot{a}_1 \\ \dot{a}_2 \\ \dot{a}_3 \end{bmatrix} \approx \frac{\epsilon \theta^2}{\theta^2 + k_3^2} \begin{bmatrix} 0 & 0 & -6 \cos t^* \sin t^* \\ 0 & 0 & 4 \cos^2 t^* - 2 \sin^2 t^* \\ 0 & -2 & 0 \end{bmatrix} \begin{bmatrix} a_1 \\ a_2 \\ a_3 \end{bmatrix}, \quad (21)$$

We keep in mind from the definition that $k_3 = 1 - 2\epsilon \theta \cos t^* \approx 0$ or $\cos t^* \approx 1/(2\epsilon \theta)$.

We can make a crude estimate, based on (21), of how the velocity amplitude $\mathbf{a}(t)$ is amplified during the short time interval around $t = t^*$. Define the local time α around t^* by $t = t^* + \alpha$. Then $k_3 = 1 - 2\epsilon \theta \cos(t^* + \alpha)$ is expanded in a power series in α as

$$k_3 = 1 - 2\epsilon \theta \cos(t^* + \alpha) = 2\epsilon \theta \sin t^* \alpha + \frac{1}{2} \alpha^2 + O(\alpha^3). \quad (22)$$

From $\epsilon \theta \cos t^* = 1/2$, $\sin t^* = \sqrt{1 - 1/(4\epsilon^2 \theta^2)}$. The integration range is $t^* - \delta t < t^* + \alpha < t^* + \delta t$, or $-\delta t < \alpha < \delta t$, for a short but sufficient time interval $2\delta t$ for the drastic amplification process to be completed.

Once the largest eigenvalue $\lambda(t)$ is found, the velocity amplitude is estimated from above as $|\mathbf{a}(t)| \leq e^{\int_{-\delta t}^{\delta t} \lambda_1 d\alpha} |\mathbf{a}(0)|$. This rapid amplification takes place at the two short intervals around t^* during one period T . To translate this short-time interval analysis into the Floquet exponent, it suffices to calculate

$$\sigma = 2 \int_{-\delta t}^{\delta t} \lambda(t) dt / T, \quad (23)$$

where λ is the largest eigenvalue.

In view of equation (21) for $|k_3| \ll \theta$ in the immediate neighborhood of $t = t^*$, the eigenvalue $\lambda(t)$ could be of the same order as

$$\lambda \approx C \frac{|\epsilon| \theta^2}{\theta^2 + k_3^2}, \quad (24)$$

for some constant C , $C = 2$ say. We retain $k_3 \approx 2\epsilon\theta \sin t^* \alpha$ to first order in α for $|\alpha| \ll 1$, and evaluate the integral $\int_{-\delta t}^{\delta t} \lambda dt$ in the following way,

$$\int_{-\delta t}^{\delta t} \lambda dt \approx C |\epsilon| \theta^2 \int_{-\delta t}^{\delta t} \frac{d\alpha}{\theta^2 + 4\epsilon^2 \theta^2 \sin^2 t^* \alpha^2} = \frac{C}{4|\epsilon| \sin^2 t^*} \int_{-\delta t}^{\delta t} \frac{d\alpha}{\alpha^2 + \frac{1}{4\epsilon^2 \sin^2 t^*}}. \quad (25)$$

According to our numerical solution, $\epsilon\theta$, with θ for the maximum amplification, is some finite value around 3 or 4 in $\sin t^* \approx \sqrt{1 - 1/(4\epsilon^2 \theta^2)}$, it follows that $1/(4\epsilon^2 \sin^2 t^*) \ll 1$ for $|\epsilon| \gg 1$. The integral in (25) is evaluated as

$$\int_{-\delta t}^{\delta t} \frac{d\alpha}{\alpha^2 + \frac{1}{4\epsilon^2 \sin^2 t^*}} \approx 2|\epsilon| \pi \sin t^*, \quad (26)$$

for $\delta t \gg 1/(2|\epsilon| \sin t^*)$. Note that δt may be very small value for $|\epsilon| \gg 1$. Consequently

$$\int_{-\delta t}^{\delta t} \lambda d\alpha \approx \frac{C\pi}{2 \sin t^*}. \quad (27)$$

As $\sin t^*$ is close to 1, the Floquet exponent could be finite in the limit of $|\epsilon| \rightarrow \infty$.

As an illustration, we choose a large value $\epsilon = 100$, for which $\theta \approx 0.011916\pi$ for the maximum growth rate as is seen from figure 4. Thus $\epsilon\theta \approx 3.74352$, and, with the choice of $C = 2$ for instance, we have

$$\int_{-\delta t}^{\delta t} \lambda d\alpha \approx 3.19865, \quad e^{\int_{-\delta t}^{\delta t} \lambda d\alpha} \approx e^{3.19865} \approx 24.4995, \quad (28)$$

which is not very different from the numerical solution (figures 5 and 6). The contribution to the Floquet exponent is

$$2 \int_{t^* - \delta t}^{t^* + \delta t} \lambda dt / T \approx (2 \times 3.19865) / 2\pi = 1.01816. \quad (29)$$

This value accounts for a substantial part of the growth rate $\sigma = 1.70144$ for $\epsilon = 100$ (see figure 3).

For reference, we make the estimation of a possible contribution from the term including k_3 in eigenvalue λ of equation (17).

$$\int_{-\delta t}^{\delta t} \frac{|k_3|}{\theta^2 + k_3^2} d\alpha = 2 \int_0^{\delta t} \frac{2|\epsilon| \theta \sin t^* \alpha}{\theta^2 + 4\epsilon^2 \theta^2 \sin^2 t^* \alpha^2} d\alpha. \quad (30)$$

After integration, we get

$$\int_{-\delta t}^{\delta t} \frac{|k_3|}{\theta^2 + k_3^2} d\alpha = \frac{1}{|\epsilon| \theta \sin t^*} \log(|\epsilon| \sin t^* \delta t). \quad (31)$$

This may bring in logarithmic divergence, in ϵ , of the Floquet exponent. However the relevant contribute would not be equation (31) but $\int_{-\delta t}^{\delta t} k_3/(k_3^2 + \theta^2) d\alpha = 0$.

5. Comparison with the case of Mahalov's flow

Let us compare the solution of the amplitude equations of Mahalov's and Kerswell's flows for large value of precession frequency $|\epsilon|$. The numerical computation tells us that, for Mahalov's flow, we can restrict the inclination angle to $\theta = 0$ at which the maximum growth rate is attained in the limit of $|\epsilon| \rightarrow \infty$ (Me Me Naing and Fukumoto 2009). With this restriction, the wave vector and the amplitude equations of Mahalov's flow approaches, for $|\epsilon|^g g1$.

$$\mathbf{k} = (-2\epsilon, 0, 1), \quad (32)$$

and

$$\begin{bmatrix} \dot{a}_1 \\ \dot{a}_2 \\ \dot{a}_3 \end{bmatrix} \approx \frac{1}{4\epsilon^2} \begin{bmatrix} 0 & 1 & 0 \\ -4\epsilon^2 - 1 & 0 & 2\epsilon(4\epsilon^2 + 1) \\ 0 & 2\epsilon & 0 \end{bmatrix} \begin{bmatrix} a_1 \\ a_2 \\ a_3 \end{bmatrix}. \quad (33)$$

We exemplify in figure 7 the temporal evolution of $a_2(t)$ ($0 \leq t \leq 2\pi$) for the initial condition $\mathbf{a}(0) = (0, 1, 0)$.

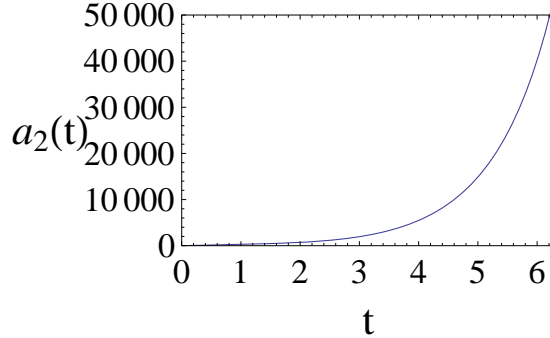


Figure 7. The y component of the solution of equation (33) for $\epsilon = 100$ and $\theta = 0$.

The solution grows exponentially, in striking contrast with Kerswell's flow (figures 5 and 6).

To gain an insight into behavior of this simple exponential growth, we deduce the solution of equation (33) for $|\epsilon| \gg 1$. In this regime, (33) simplifies to

$$\begin{bmatrix} \dot{a}_1 \\ \dot{a}_2 \\ \dot{a}_3 \end{bmatrix} \approx \begin{bmatrix} 0 & 0 & 0 \\ -1 & 0 & 2\epsilon \\ 0 & \frac{1}{2\epsilon} & 0 \end{bmatrix} \begin{bmatrix} a_1 \\ a_2 \\ a_3 \end{bmatrix}. \quad (34)$$

The general solution of equation (34) is

$$a_1 = C_1, \quad a_2 = C_2 e^t + C_3 e^{-t}, \quad a_3 = (C_1 + C_2 e^t - C_3 e^{-t})/2\epsilon, \quad (35)$$

where C_1 , C_2 and C_3 are arbitrary constants. This solution indicates that the growth rate is

$$\sigma = 1. \quad (36)$$

We see from figure 7 for $a_2(t)$ ($0 \leq t \leq 2\pi$) that the amplitude grows monotonically. By contrast, in the case of Kerswell's flow, the amplitude grows explosively for very short time intervals around the time of $k_3 = 0$ for very small but non-zero θ in the limit of $|\epsilon| \rightarrow \infty$ (figures 5 and 6). Here we remark that the growth rate is $\sigma = 0$ for $\theta = 0$ for the case of Kerswell's flow. Taking $\theta = 0$ for $|\epsilon| \gg 1$, equation (7) becomes $\mathbf{k} = (0, 0, 1)$ and equation (6) is written as

$$\begin{bmatrix} \dot{a}_1 \\ \dot{a}_2 \\ \dot{a}_3 \end{bmatrix} = \begin{bmatrix} 0 & 1 & 0 \\ -1 & 0 & 4\epsilon \\ 0 & 0 & 0 \end{bmatrix} \begin{bmatrix} a_1 \\ a_2 \\ a_3 \end{bmatrix}. \quad (37)$$

The general solution of equation (37) is

$$a_1 = c_1 \sin t - 4\epsilon c_3, \quad a_2 = c_1 \cos t, \quad a_3 = c_3, \quad (38)$$

where c_1 , c_2 and c_3 are arbitrary constants. This solution indicates that the growth rate is $\sigma = 0$. The result of §4 demonstrates that, for $|\epsilon| \gg 1$, the behavior of the solution with small but non-zero θ is totally different from that with $\theta = 0$. The maximum growth rate is discontinuous with respect to θ at $\theta = 0$ in the limit of $|\epsilon| \rightarrow \infty$.

Mahalov's and Kerswell's flows are rotating flows subjected to the same form of precessional perturbation and the difference lies only in the linear shear flow induced by the perturbation. It is revealed that the occurrence of $k_3 = 0$ brings about singular behaviour, while that a smooth exponential-type growth is realized in the absence of moments of $k_3 = 0$.

6. Conclusion

We have studied the stability of precessing rotating flows with respect to short-wave three-dimensional disturbances by adopting the geometrical optics technique. This technique converts the partial differential equations for linear hydrodynamic stability into a system of ordinary differential equations, or the characteristic equations. There are two steady solutions, Mahalov's and Kerswell's flows, linear in coordinates relative to the rotating frame, of the Euler equations for motion of rigid-body rotation subject to precession, of frequency ϵ , about the axis normal to the axis of rigid-body rotation. For a rotating basic flow with closed streamlines, these equations have coefficients periodic in time, and are amenable to the Floquet theory. The resulting matrix eigenvalue problem has been solved numerically for arbitrary values of $|\epsilon|$, and asymptotically for $|\epsilon| \ll 1$ and for $|\epsilon| \gg 1$.

For small values of the precession frequency $|\epsilon|$, the set of the characteristic equations are reduced to the Mathieu equation for any value of θ , the tilting angle of wave vector from the z -axis, for Mahalov's flow and except for values of θ close to $\pi/2$ for Kerswell's flow. Although the appearances of Mahalov's and Kerswell's flows are different, the growth rate takes a common value $\sigma = 5\sqrt{15}\epsilon/32$, to leading order in ϵ , and the instability of precession origin was identified. We remark that this primary instability mode shares a common mathematical structure also with the curvature instability of a vortex ring (Hattori and Fukumoto 2003, Fukumoto and Hattori 2005). A distinction makes its appearance between Mahalov's and Kerswell's flows when we enter into the region of large precessional frequency $|\epsilon|$. For Kerswell's flow, the growth rate exceeds angular velocity of the basic rotation and increases monotonically with $|\epsilon|$, which surpasses Mahalov's flows. For the latter, $\sigma = 1$, the angular velocity of the basic flow rotation, in the limit of $|\epsilon| \rightarrow \infty$. A novel feature of the disturbance growth for Kerswell's flow is drastic amplification of disturbance for a very short time around the moment of $k_3 = 0$. This happens to be the reason why the reduction method of Bayly *et al.* (1996) is permitted.

Recently, global stability analysis has been developed and has been extended to weakly nonlinear regime for the elliptical instability (Mason and Kerswell 1999, Fukumoto *et al.* 2005, Rodrigues and Luca 2009) and for the precessional instability with no strain (Mason and Kerswell 2002, Meunier *et al.* 2008). The nonlinear interaction of disturbances, the modification of mean flow by the nonlinear and the boundary layer effects, and the viscous dissipation may significantly alter the evolution of linearly excited waves. The nonlinear excitation of waves via the secondary and the tertiary instability brings in chaotic behavior of rotating flows and in transition to turbulence (Mason and Kerswell 1999, Mason and Kerswell 2002, Fukumoto *et al.* 2005). This paper suggests a rich behavior of unstable waves on a precessing rotating flow of arbitrary precession frequency, but the knowledge has been limited to the linear, in amplitude, regime. The nonlinear stage of evolution of excited waves calls for an individual investigation.

6.1. Acknowledgments

M. M. N. would like to express her deep appreciation to the Ministry of Education, Culture, Sports, Science and Technology, Japan for financial support with scholarship award. Y. F. was supported in part by a Grant-in-Aid for Scientific Research from the Japan Society of Promotion of Science (Grant No. 21540390).

References

- Bayly B J 1986 Three-dimensional instability of elliptical flow *Phys. Rev. Lett.* **57** 2160-2163
- Bayly B J, Holm D D and Lifschitz A 1996 Three-dimensional stability of elliptical vortex columns in external strain flows *Philos. Trans. R. Soc. Lond. A* **354** 895-926

- Craik A D D 1989 The stability of unbounded two- and three- dimensional flows subject to body forces: some exact solutions *J. Fluid Mech.* **198** 275-292
- Friedlander S and Vishik M M 1991 Instability criteria for the flow of an inviscid incompressible fluid *Phys. Rev. Lett.* **66** 2204-2206
- Fukumoto Y and Hattori Y 2005 Curvature instability of a vortex ring *J. Fluid Mech.* **526** 77-115
- Fukumoto Y, Hattori Y and Fujimura K 2005 in *Proc. 3rd Int. Conf. Vortex Flows and Vortex Models*, ed. K. Kamemoto (Japan Society of Mechanical Engineers) p 149
- Fukumoto Y and Miyazaki T 1996 Local stability of two-dimensional steady irrotational solenoidal flows with closed streamlines *J. Phys. Soc. Jpn.* **65** 107-113
- Goto F, Ishii N, Kida S and Nishioka M 2007 Turbulence generator using a precessing sphere *Phys. Fluids* **19**, 061705
- Hattori Y and Fukumoto Y 2003 Short-wavelength stability analysis of thin vortex rings *Phys. Fluids* **15** 3151-3163
- Ince E L 1956 *Ordinary Differential Equations* (Dover Publications, New York) p 384
- Kerswell R R 1993 The instability of precessing flow *Geophys. Astrophys. Fluid Dyn.* **72** 107-144
- Lifschitz A 1994 On the instability of certain motions of an ideal incompressible fluid *Advances in Applied Mathematics* **15** 404-436
- Lifschitz A and Hameiri E 1991 Local stability conditions in fluid dynamics *Phys. Fluids A* **3** 2644-2651
- Mahalov A 1993 The instability of rotating fluid columns subjected to a weak external Coriolis force *Phys. Fluids* **5** 891-900
- Mason D M and Kerswell R R 1999 Nonlinear evolution of the elliptical instability *J. Fluid Mech.* **396** 73-108
- Mason D M and Kerswell R R 2002 Chaotic dynamics in a strained rotating flow: a precessing plane fluid layer *J. Fluid Mech.* **471** 71-106
- Me Me Naing and Fukumoto Y 2009 Local instability of an elliptical flow subjected to a Coriolis Force *J. Phys. Soc. Jpn.* **78** 124401
- Meunier P, Eloy C, Lagrange R and Nadal F 2008 A rotating fluid cylinder subject to weak precession *J. Fluid Mech.* **599** 405-440
- Miyazaki T 1993 Elliptical instability in a stably stratified rotating fluid *Phys. Fluids A* **5** 2702-2709
- Rodrigues S B and Luca J D 2009 Weakly nonlinear analysis of short-wave elliptical instability *Phys. Fluids* **21** 014108
- Waleffe F 1990 On the three-dimensional instability of strained vortices *Phys. Fluids A* **2**, 76-80

List of MI Preprint Series, Kyushu University

The Global COE Program
Math-for-Industry Education & Research Hub

MI

- MI2008-1 Takahiro ITO, Shuichi INOKUCHI & Yoshihiro MIZOGUCHI
Abstract collision systems simulated by cellular automata
- MI2008-2 Eiji ONODERA
The initial value problem for a third-order dispersive flow into compact almost Hermitian manifolds
- MI2008-3 Hiroaki KIDO
On isosceles sets in the 4-dimensional Euclidean space
- MI2008-4 Hirofumi NOTSU
Numerical computations of cavity flow problems by a pressure stabilized characteristic-curve finite element scheme
- MI2008-5 Yoshiyasu OZEKI
Torsion points of abelian varieties with values in infinite extensions over a p-adic field
- MI2008-6 Yoshiyuki TOMIYAMA
Lifting Galois representations over arbitrary number fields
- MI2008-7 Takehiro HIROTSU & Setsuo TANIGUCHI
The random walk model revisited
- MI2008-8 Silvia GANDY, Masaaki KANNO, Hirokazu ANAI & Kazuhiro YOKOYAMA
Optimizing a particular real root of a polynomial by a special cylindrical algebraic decomposition
- MI2008-9 Kazufumi KIMOTO, Sho MATSUMOTO & Masato WAKAYAMA
Alpha-determinant cyclic modules and Jacobi polynomials

- MI2008-10 Sangyeol LEE & Hiroki MASUDA
Jarque-Bera Normality Test for the Driving Lévy Process of a Discretely Observed Univariate SDE
- MI2008-11 Hiroyuki CHIHARA & Eiji ONODERA
A third order dispersive flow for closed curves into almost Hermitian manifolds
- MI2008-12 Takehiko KINOSHITA, Kouji HASHIMOTO and Mitsuhiro T. NAKAO
On the L^2 a priori error estimates to the finite element solution of elliptic problems with singular adjoint operator
- MI2008-13 Jacques FARAUT and Masato WAKAYAMA
Hermitian symmetric spaces of tube type and multivariate Meixner-Pollaczek polynomials
- MI2008-14 Takashi NAKAMURA
Riemann zeta-values, Euler polynomials and the best constant of Sobolev inequality
- MI2008-15 Takashi NAKAMURA
Some topics related to Hurwitz-Lerch zeta functions
- MI2009-1 Yasuhide FUKUMOTO
Global time evolution of viscous vortex rings
- MI2009-2 Hidetoshi MATSUI & Sadanori KONISHI
Regularized functional regression modeling for functional response and predictors
- MI2009-3 Hidetoshi MATSUI & Sadanori KONISHI
Variable selection for functional regression model via the L_1 regularization
- MI2009-4 Shuichi KAWANO & Sadanori KONISHI
Nonlinear logistic discrimination via regularized Gaussian basis expansions
- MI2009-5 Toshiro HIRANOUCI & Yuichiro TAGUCHI
Flat modules and Groebner bases over truncated discrete valuation rings

- MI2009-6 Kenji KAJIWARA & Yasuhiro OHTA
Bilinearization and Casorati determinant solutions to non-autonomous 1+1 dimensional discrete soliton equations
- MI2009-7 Yoshiyuki KAGEI
Asymptotic behavior of solutions of the compressible Navier-Stokes equation around the plane Couette flow
- MI2009-8 Shohei TATEISHI, Hidetoshi MATSUI & Sadanori KONISHI
Nonlinear regression modeling via the lasso-type regularization
- MI2009-9 Takeshi TAKAISHI & Masato KIMURA
Phase field model for mode III crack growth in two dimensional elasticity
- MI2009-10 Shingo SAITO
Generalisation of Mack's formula for claims reserving with arbitrary exponents for the variance assumption
- MI2009-11 Kenji KAJIWARA, Masanobu KANEKO, Atsushi NOBE & Teruhisa TSUDA
Ultradiscretization of a solvable two-dimensional chaotic map associated with the Hesse cubic curve
- MI2009-12 Tetsu MASUDA
Hypergeometric q -functions of the q -Painlevé system of type $E_8^{(1)}$
- MI2009-13 Hidenao IWANE, Hitoshi YANAMI, Hirokazu ANAI & Kazuhiro YOKOYAMA
A Practical Implementation of a Symbolic-Numeric Cylindrical Algebraic Decomposition for Quantifier Elimination
- MI2009-14 Yasunori MAEKAWA
On Gaussian decay estimates of solutions to some linear elliptic equations and its applications
- MI2009-15 Yuya ISHIHARA & Yoshiyuki KAGEI
Large time behavior of the semigroup on L^p spaces associated with the linearized compressible Navier-Stokes equation in a cylindrical domain

- MI2009-16 Chikashi ARITA, Atsuo KUNIBA, Kazumitsu SAKAI & Tsuyoshi SAWABE
Spectrum in multi-species asymmetric simple exclusion process on a ring
- MI2009-17 Masato WAKAYAMA & Keitaro YAMAMOTO
Non-linear algebraic differential equations satisfied by certain family of elliptic functions
- MI2009-18 Me Me NAING & Yasuhide FUKUMOTO
Local Instability of an Elliptical Flow Subjected to a Coriolis Force
- MI2009-19 Mitsunori KAYANO & Sadanori KONISHI
Sparse functional principal component analysis via regularized basis expansions and its application
- MI2009-20 Shuichi KAWANO & Sadanori KONISHI
Semi-supervised logistic discrimination via regularized Gaussian basis expansions
- MI2009-21 Hiroshi YOSHIDA, Yoshihiro MIWA & Masanobu KANEKO
Elliptic curves and Fibonacci numbers arising from Lindenmayer system with symbolic computations
- MI2009-22 Eiji ONODERA
A remark on the global existence of a third order dispersive flow into locally Hermitian symmetric spaces
- MI2009-23 Stjepan LUGOMER & Yasuhide FUKUMOTO
Generation of ribbons, helicoids and complex scherk surface in laser-matter Interactions
- MI2009-24 Yu KAWAKAMI
Recent progress in value distribution of the hyperbolic Gauss map
- MI2009-25 Takehiko KINOSHITA & Mitsuhiro T. NAKAO
On very accurate enclosure of the optimal constant in the a priori error estimates for H_0^2 -projection

- MI2009-26 Manabu YOSHIDA
Ramification of local fields and Fontaine's property (Pm)
- MI2009-27 Yu KAWAKAMI
Value distribution of the hyperbolic Gauss maps for flat fronts in hyperbolic three-space
- MI2009-28 Masahisa TABATA
Numerical simulation of fluid movement in an hourglass by an energy-stable finite element scheme
- MI2009-29 Yoshiyuki KAGEI & Yasunori MAEKAWA
Asymptotic behaviors of solutions to evolution equations in the presence of translation and scaling invariance
- MI2009-30 Yoshiyuki KAGEI & Yasunori MAEKAWA
On asymptotic behaviors of solutions to parabolic systems modelling chemotaxis
- MI2009-31 Masato WAKAYAMA & Yoshinori YAMASAKI
Hecke's zeros and higher depth determinants
- MI2009-32 Olivier PIRONNEAU & Masahisa TABATA
Stability and convergence of a Galerkin-characteristics finite element scheme of lumped mass type
- MI2009-33 Chikashi ARITA
Queueing process with excluded-volume effect
- MI2009-34 Kenji KAJIWARA, Nobutaka NAKAZONO & Teruhisa TSUDA
Projective reduction of the discrete Painlevé system of type $(A_2 + A_1)^{(1)}$
- MI2009-35 Yosuke MIZUYAMA, Takamasa SHINDE, Masahisa TABATA & Daisuke TAGAMI
Finite element computation for scattering problems of micro-hologram using DtN map

- MI2009-36 Reiichiro KAWAI & Hiroki MASUDA
Exact simulation of finite variation tempered stable Ornstein-Uhlenbeck processes
- MI2009-37 Hiroki MASUDA
On statistical aspects in calibrating a geometric skewed stable asset price model
- MI2010-1 Hiroki MASUDA
Approximate self-weighted LAD estimation of discretely observed ergodic Ornstein-Uhlenbeck processes
- MI2010-2 Reiichiro KAWAI & Hiroki MASUDA
Infinite variation tempered stable Ornstein-Uhlenbeck processes with discrete observations
- MI2010-3 Kei HIROSE, Shuichi KAWANO, Daisuke MIIKE & Sadanori KONISHI
Hyper-parameter selection in Bayesian structural equation models
- MI2010-4 Nobuyuki IKEDA & Setsuo TANIGUCHI
The Itô-Nisio theorem, quadratic Wiener functionals, and 1-solitons
- MI2010-5 Shohei TATEISHI & Sadanori KONISHI
Nonlinear regression modeling and detecting change point via the relevance vector machine
- MI2010-6 Shuichi KAWANO, Toshihiro MISUMI & Sadanori KONISHI
Semi-supervised logistic discrimination via graph-based regularization
- MI2010-7 Teruhisa TSUDA
UC hierarchy and monodromy preserving deformation
- MI2010-8 Takahiro ITO
Abstract collision systems on groups
- MI2010-9 Hiroshi YOSHIDA, Kinji KIMURA, Naoki YOSHIDA, Junko TANAKA & Yoshihiro MIWA
An algebraic approach to underdetermined experiments

- MI2010-10 Kei HIROSE & Sadanori KONISHI
Variable selection via the grouped weighted lasso for factor analysis models
- MI2010-11 Katsusuke NABESHIMA & Hiroshi YOSHIDA
Derivation of specific conditions with Comprehensive Groebner Systems
- MI2010-12 Yoshiyuki KAGEI, Yu NAGAFUCHI & Takeshi SUDOU
Decay estimates on solutions of the linearized compressible Navier-Stokes equation around a Poiseuille type flow
- MI2010-13 Reiichiro KAWAI & Hiroki MASUDA
On simulation of tempered stable random variates
- MI2010-14 Yoshiyasu OZEKI
Non-existence of certain Galois representations with a uniform tame inertia weight
- MI2010-15 Me Me NAING & Yasuhide FUKUMOTO
Local Instability of a Rotating Flow Driven by Precession of Arbitrary Frequency